ISSN 1392–1320 MATERIALS SCIENCE (MEDŽIAGOTYRA). Vol. 14, No. 2. 2008

Effects of Solution Concentration on the Properties of Cu_4SnS_4 Thin Films

Kassim ANUAR[1*], Soon Min HO[1], Wee Tee TAN[1], Mohd. Sharif ATAN[1], Dzulkefly KUANG[1], Haron MD. JELAS[1], Nagalingam SARAVANAN[2]

[1]*Department of Chemistry, Faculty of Science, University Putra Malaysia, 43400 Serdang, Selangor, Malaysia*
[2]*Faculty of Engineering and Science, University Tunku Abdul Rahman, 53300 Kuala Lumpur, Malaysia*

Received 25 April 2008; accepted 08 June 2008

Copper tin sulfide thin films were electrodeposited on the indium tin oxide substrate from an aqueous solution containing $CuSO_4$, $SnCl_2$ and $Na_2S_2O_3$ at pH 1. Deposition at various concentrations was attempted in order to study the effect of electrolytes concentration on the film properties. The thin films were characterized using X-ray diffraction and atomic force microscopy. The absorption properties, band gap energy and transition type was determined using UV-Vis Spectrophotometer. The thin films produced were polycrystalline in nature. The XRD data showed that the most intense peak is at $2\theta = 30.2°$ which belongs to (221) plane of Cu_4SnS_4. The AFM images indicated that the lower concentration leads to smaller crystal size, as well as higher optical absorption values. The optimum bath composition was found to be 0.01 M for $CuSO_4$, $Na_2S_2O_3$ and $SnCl_2$. The band gap value was found to be 1.7 eV with indirect transition.
Keywords: bandgap energy, electrodeposition, semiconducting material, solar cells, thin films.

INTRODUCTION

The conversion of sunlight directly into electricity using the electronic properties of suitable materials is one of the most elegant energy conversion processes. The solar cell technology has been enormous development during the last three decades, initially for providing electrical power for spacecrafts and more recently for terrestrial applications. The present solar cells industry is dominated by crystalline silicone based solar cells. However, silicon supply is the problem limiting the future of their market. Thin film solar cells, which need merely a very thin semiconductor film have advantages in the lowering the material cost.

There are many methods for preparing thin films such as chemical bath deposition [1], vacuum evaporation [2], electrodeposition [3], molecular beam epitaxy [4], close spaced sublimation [5], thermal evaporation [6], spray pyrolysis [7], sputter deposition [8], metal organic chemical vapor deposition [9] and plasma-enhanced chemical vapor deposition [10]. Amongst these deposition methods, electrodeposition is more attractive, since it offers the advantages of simplicity, economy, convenience and several experimental parameters can be controlled more precisely. To this date, many semiconductor thin films deposited by electrodeposition have been reported including Cu_2S [11], SnS [12], CdSe [13], CdS [14], PbS [15], PbSe [16], SnSe [17], ZnS [18], $CdIn_2Se_4$ [19], ZnCuTe [20], $SnS_{0.5}Se_{0.5}$ [21], $CuInS_2$ [22] and $CuInSe_2$ [23].

In this paper, we report the morphological, structural and optical properties of Cu_4SnS_4 thin films obtained by electrodeposition method at various concentrations of $CuSO_4$, $SnCl_2$ and $Na_2S_2O_3$. The films have been characterized by X-Ray Diffraction for structure determination, atomic force microscope for surface morphology study and UV-Visible Spectrophotometer for optical absorption properties study.

*Corresponding author. Tel.: +603-89466779; fax.: +603-89435380.
E-mail address: *anuar@fsas.upm.edu.my* (K. Anuar)

EXPERIMENTAL PROCEDURE

The electrodeposition was carried out in a conventional three-electrode cell. The indium-doped tin oxide (ITO) was used as the working electrode. The counter electrode and reference electrode was made from platinum wire and Ag/AgCl, respectively. The ITO was cleaned ultrasonically in ethanol and distilled water before use. The EG&G Princeton Applied Research potentiostat driven by a software model 270 Electrochemical Analysis System was used to control electrodeposition process and to monitor current and voltage profiles. The solutions used were $CuSO_4$, $SnCl_2$, $Na_2S_2O_3$ and HCl. The experiment was performed at room temperature without stirring. The pH was maintained at 1 using 0.05 M of HCl. HCl was added to prevent the formation of hydroxyl species and insoluble compounds. Also, HCl used to completely dissolve the tin chloride to result in a clear transparent solution. In order to investigate the effect of electrolytes concentration on the film properties, deposition at various concentrations was carried out. The first set of experiment was carried out using constant concentration of 0.01 M of $CuSO_4$, $SnCl_2$ and varying concentrations of $Na_2S_2O_3$ (0.01 M – 0.02 M) solutions. The second set of experiment was carried out using fixed concentration of 0.01 M of $CuSO_4$, $Na_2S_2O_3$ and varying concentrations of $SnCl_2$ (0.01 M – 0.02 M) solutions. The third set of experiment was carried out using constant concentration of 0.01 M of $SnCl_2$, $Na_2S_2O_3$ and varying concentrations of $CuSO_4$ (0.01 M – 0.02 M) solutions. The deposition was carried out at –600 mV vs. Ag/AgCl for 45 minutes. After the deposition, the films were washed with distilled water and kept for analysis.

X-ray diffraction (XRD) analysis was carried out, using a Philips PM 11730 diffractometer for the 2θ ranging from 25° to 60° with CuK_α ($\lambda = 1.5418$ Å) radiation. Topography was measured by using an atomic force microscopy (Quesant Instrument Corporation, Q-Scope 250) operating in contact mode, with Si_3N_4 cantilever. The photoelectrochemical experiments were performed in

$[Fe(CN)_6]^{3-}/[Fe(CN)_6]^{4-}$ redox system by running linear sweep voltammetry (LSV) between two potentials limits (1.0 V to –1.0 V). The sequence of constant illumination, chopped illumination and dark period were performed on the PEC cell to study the effect on photoactivity behavior. A halogen lamp (300 W, 120 V) was used for illuminating the electrode. Optical absorption study was carried out using the Perkin Elmer UV/Vis Lambda 20 Spectrophotometer. The film-coated indium doped tin oxide (ITO) glass was placed across the sample radiation pathway while the uncoated ITO glass was put across the reference path. The absorption data were manipulated for the determination of the band gap energy, E_g.

RESULTS AND DISCUSSIONS

Fig. 1 shows the XRD patterns of the films deposited at various $CuSO_4$ concentrations (0.01 M – 0.02 M) and constant $Na_2S_2O_3$, $SnCl_2$ at 0.01 M. There are six Cu_4SnS_4 peaks at $2\theta = 28.6°$, 30.1°, 35.2°, 42.9°, 45.2° and 50.6° for the samples prepared at 0.01 M, 0.015 M and 0.02 M of $CuSO_4$. The corresponding interplanar distances are well in agreement with JCPDS data (Reference code: 010710129) of 3.12, 2.96, 2.54, 2.10, 2.00 and 1.80 Å, which attributed to the (102), (221), (420), (331), (512) and (711) planes, respectively. All these peaks are related to the compound of Cu_4SnS_4 of orthorhombic structure (a = 13.5580 Å, b = 7.6810 Å, c = 6.4120 Å, $\alpha = \beta = \gamma = 90°$). However, as the concentration of $CuSO_4$ was higher than 0.015 M and 0.02 M, the copper sulfide peaks (Reference code: 000653556) which corresponding to 2.82 Å and 2.32 Å at $2\theta = 31.8°$ and 38.8°, respectively were obtained.

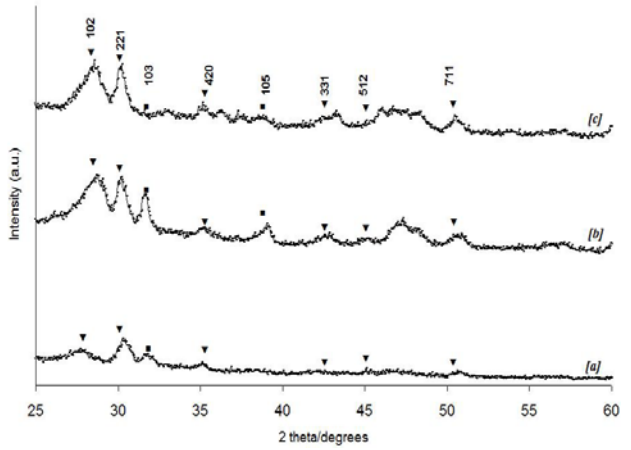

Fig. 1. XRD patterns of samples prepared at various $CuSO_4$ concentrations: a – 0.01 M; b – 0.015 M; c – 0.02 M. Concentration of $SnCl_2$ and $Na_2S_2O_3$ are fixed at 0.01 M. Cu_4SnS_4 – ▲; CuS – ■

Fig. 2 shows the XRD patterns of the films deposited at various $SnCl_2$ concentrations (0.01 M – 0.02 M) and fixed $Na_2S_2O_3$, $CuSO_4$ at 0.01 M. XRD indicates the presence of six peaks at $2\theta = 28.5°$, 30.1°, 35.1°, 42.8, 45.2° and 50.5° belonging to Cu_4SnS_4 for samples prepared using lower concentrations (0.01 M and 0.015 M). There is no copper sulfide peaks were observed from the samples deposited with 0.01 M of tin chloride. Six peaks corresponding to interplanar distance of 3.12, 2.96, 2.55, 2.11, 2.01 and 1.80 Å were observed for the film prepared from 0.02 M $SnCl_2$.

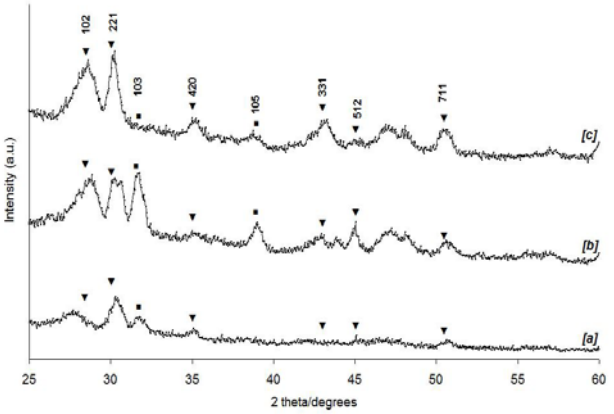

Fig. 2. XRD patterns of samples prepared at various $SnCl_2$ concentrations: a – 0.01 M; b – 0.015 M; c – 0.02 M. Concentration of $CuSO_4$ and $Na_2S_2O_3$ are fixed at 0.01 M. Cu_4SnS_4 – ▲; CuS – ■

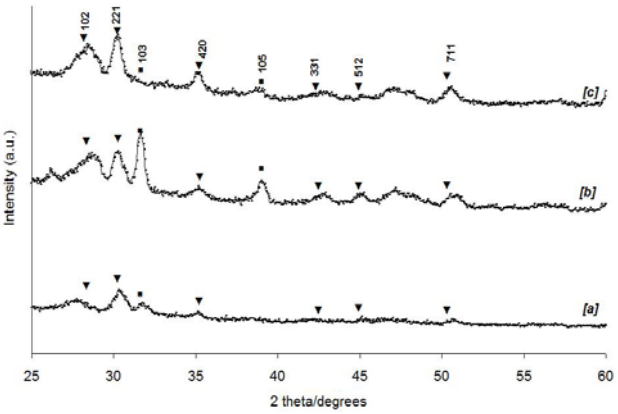

Fig. 3. XRD patterns of samples prepared at various $Na_2S_2O_3$ concentrations: a – 0.01 M; b – 0.015 M; c – 0.02 M. Concentration of $CuSO_4$ and $SnCl_2$ are fixed at 0.01 M. Cu_4SnS_4 – ▲; CuS – ■

Fig. 3 shows the XRD patterns of the films deposited at various $Na_2S_2O_3$ concentrations (0.01 M – 0.02 M) with constant $CuSO_4$, $SnCl_2$ at 0.01 M. The thin films prepared in different concentrations of $Na_2S_2O_3$ showed six peaks at $2\theta = 28.9°$, 30.1°, 35.1°, 42.8, 45.2° and 50.7°, corresponding to d-spacing values 3.08, 2.96, 2.55, 2.11, 2.01 and 1.79 Å, which attributed to the (102), (221), (420), (331), (512) and (711) planes, respectively were detected. The appearances of copper sulfide peaks were detected when the concentration of $Na_2S_2O_3$ was higher at 0.015 M and 0.02 M.

Fig. 4 shows the AFM images of films prepared at different $CuSO_4$ concentrations and constant $SnCl_2$, $Na_2S_2O_3$ at 0.01 M. The grain size for the film prepared at 0.015 M and 0.02 M are almost similar and do not much different from each other (Fig. 4, b, c). The crystal size decreases with the decrease of $CuSO_4$ concentration (Fig. 4, a).

Fig. 5 shows the AFM images of films prepared at different $SnCl_2$ concentrations and constant $Na_2S_2O_3$, $CuSO_4$ at 0.01 M. The images indicated that higher concentration of $SnCl_2$ leads to larger crystal size (Fig. 5, b, c) while lower $SnCl_2$ exhibits smaller crystal size (Fig. 5, a).

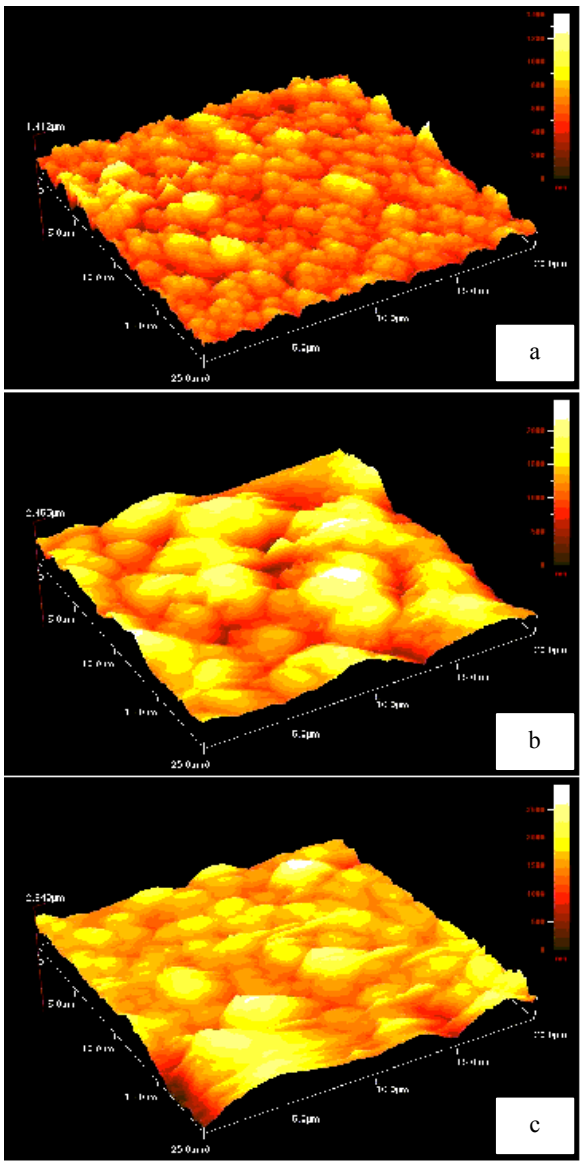

Fig. 4. Atomic force microscopy images of Cu_4SnS_4 films deposited at various $CuSO_4$ concentrations: a – 0.01 M; b – 0.015 M; c – 0.02 M. Concentration of $Na_2S_2O_3$ and $SnCl_2$ are fixed at 0.01 M

Fig. 6 shows the AFM images of films prepared at different $Na_2S_2O_3$ concentrations and constant $SnCl_2$, $CuSO_4$ at 0.01 M. The images pointed out that the deposits are crystalline and their grain size varies with the variation of $Na_2S_2O_3$ concentrations. The higher $Na_2S_2O_3$ concentration leads to bigger crystal size (Fig. 6, b, c) while lower $Na_2S_2O_3$ exhibits smaller crystal size (Fig. 6, a).

Figs. 7 – 9 shows the absorption spectra of Cu_4SnS_4 films at different concentrations of $CuSO_4$, $SnCl_2$ and $Na_2S_2O_3$, respectively. The films show a gradually increasing absorbance throughout the visible region, which makes it possible for this material to be used in a photoelectrochemical (PEC) cell. From the graph, it is indicated that the samples prepared at lower $CuSO_4$, $SnCl_2$ and $Na_2S_2O_3$ concentration (0.01 M) have higher absorption values respectively. Thus, this concentration is more preferable in the synthesis of Cu_4SnS_4 films of better quality on ITO substrate. The optical absorption values are in line with AFM results, which the larger grain size produces lower absorption results.

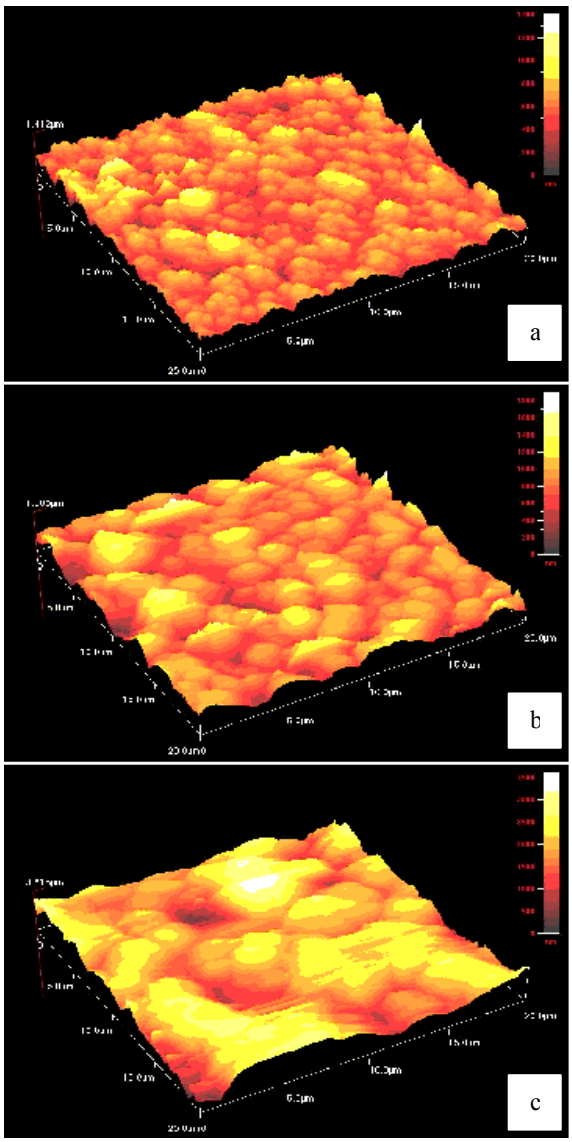

Fig. 5. Atomic force microscopy images of Cu_4SnS_4 films deposited at various $SnCl_2$ concentrations: a – 0.01 M; b – 0.015 M; c – 0.02 M. Concentration of $Na_2S_2O_3$ and $CuSO_4$ are fixed at 0.01 M

Band gap energy and transition type can be derived from mathematical treatment of data obtained from optical absorbance versus wavelength with Stern relationship of near-edge absorption:

$$A = \frac{[k(hv - E_g)^{n/2}]}{hv}, \quad (1)$$

where v is the frequency, h is the Planck's constant, k equals a constant while n carries the value of either 1 or 4. The band gap, E_g, could be obtained from a straight line plot of $(Ahv)^{2/n}$ as a function of hv. Extrapolation of the line to the base line, where the value of $(Ahv)^{2/n}$ is zero, will give E_g. The $(Ahv)^{1/2}$ versus hv plot is a straight line (Fig. 10) indicating that the energy band gap of Cu_4SnS_4 is indirect and intercept on the hv axis yield a band gap of 1.7 eV for the film prepared using 0.01 M $Na_2S_2O_3$, $SnCl_2$ and $CuSO_4$.

Fig. 11 shows the photoresponse of the Cu_4SnS_4 thin films grown from 0.01 M $CuSO_4$, $SnCl_2$ and $Na_2S_2O_3$ in contact with 0.01 M Fe^{2+}/Fe^{3+} redox couple. An increase in

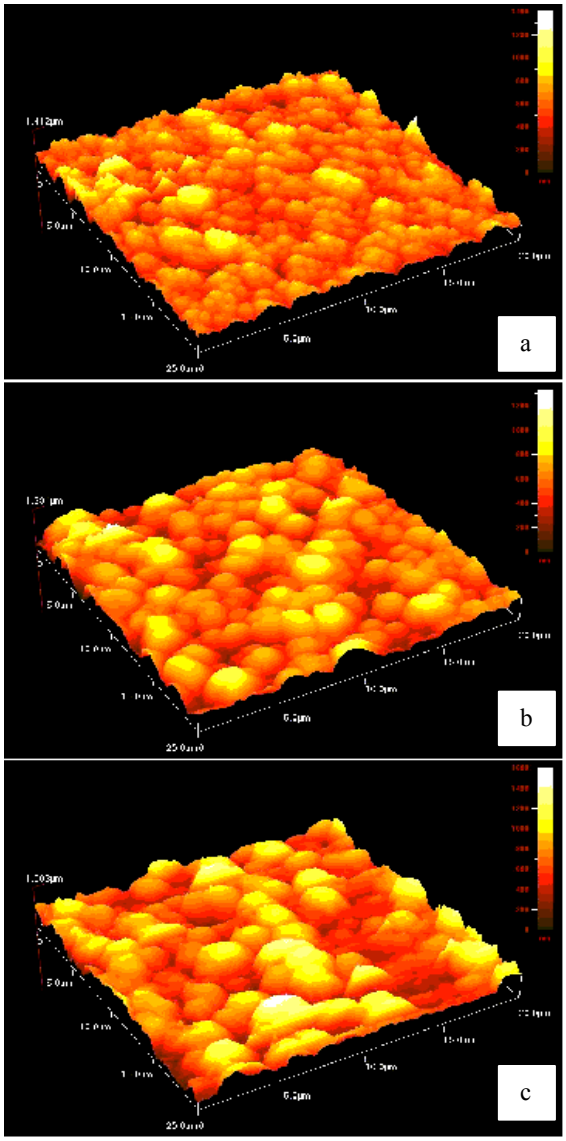

Fig. 6. Atomic force microscopy images of Cu_4SnS_4 films deposited at various $Na_2S_2O_3$ concentrations: a – 0.01 M; b – 0.015 M; c – 0.02 M. Concentration of $SnCl_2$ and $CuSO_4$ are fixed at 0.01 M

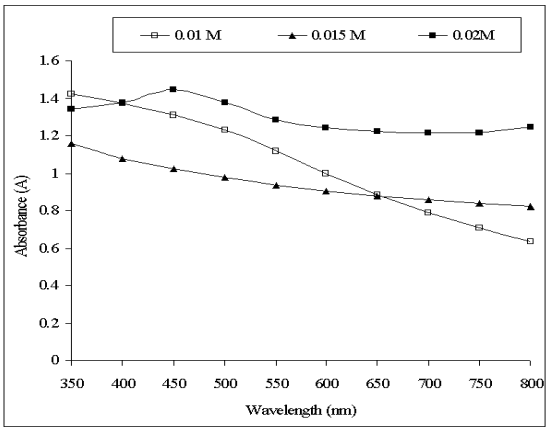

Fig. 7. Optical absorbance versus wavelength of the Cu_4SnS_4 films deposited at various $CuSO_4$ concentrations (0.01 M – 0.02 M). Concentration of $SnCl_2$ and $Na_2S_2O_3$ are fixed at 0.01 M

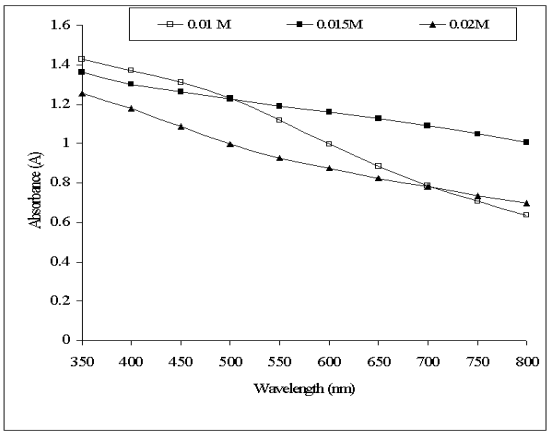

Fig. 8. Optical absorbance versus wavelength of the Cu_4SnS_4 films deposited at various $SnCl_2$ concentrations (0.01 M – 0.02 M). Concentration of $CuSO_4$ and $Na_2S_2O_3$ are fixed at 0.01 M

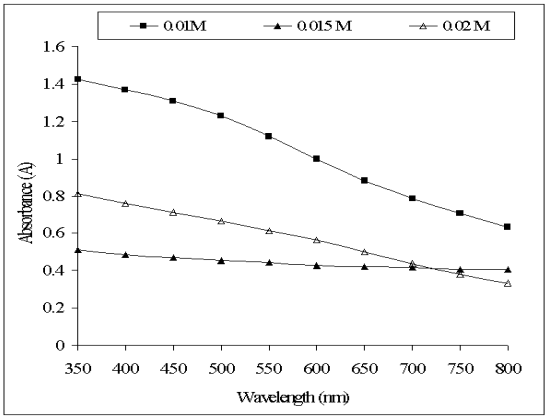

Fig. 9. Optical absorbance versus wavelength of the Cu_4SnS_4 films deposited at various $Na_2S_2O_3$ concentrations (0.01 M – 0.02 M). Concentration of $CuSO_4$ and $SnCl_2$ are fixed at 0.01 M

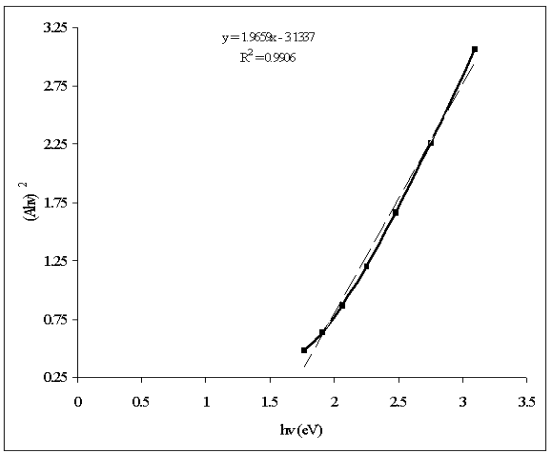

Fig. 10. Plot of $(Ahv)^{2/n}$ versus hv when n = 4 for Cu_4SnS_4 films prepared using 0.01 M $Na_2S_2O_3$, $CuSO_4$ and $SnCl_2$ solutions

current could be observed as the films were illuminated. The current change upon illumination indicates semiconductor behavior of the materials. The fact that photocurrent occurs on the positive potential region reflects that the films prepared are n-type. This indicates that the minority carriers generated are holes.

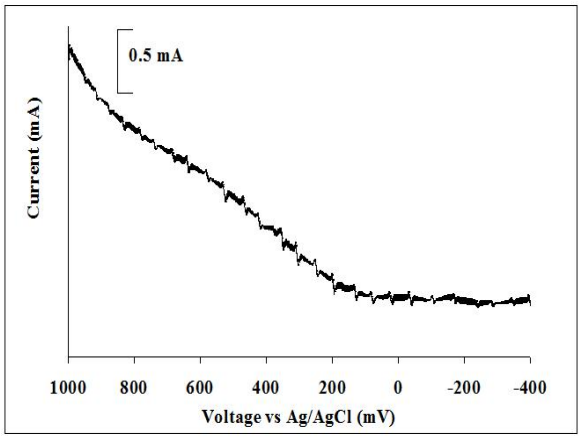

Fig. 11. The photoresponse of Cu_4SnS_4 films prepared using 0.01 M $Na_2S_2O_3$, $CuSO_4$ and $SnCl_2$ solutions

CONCLUSIONS

The Cu_4SnS_4 thin films can be electrodeposited using $CuSO_4$, $SnCl_2$ and $Na_2S_2O_3$ solution. X-ray diffraction data showed that the intensity of major peaks at 2.96 Å that attributed to (221) plane of Cu_4SnS_4. The AFM images indicated that higher $CuSO_4$, $SnCl_2$ and $Na_2S_2O_3$ concentration leads to larger crystal size. The films with smaller crystal size and show better photoresponse have been obtained from lower electrolytes concentration (0.01 M). The optimum bath composition was found to be 0.01 M for $CuSO_4$, $SnCl_2$ and $Na_2S_2O_3$ to produce good quality thin films. The films exhibited n-type semiconductor behavior with band gap energy of 1.7 eV.

Acknowledgments

The authors would like to thank the Department of Chemistry, University Putra Malaysia for the provision of laboratory facilities and MOSTI for the National Science Fellowship (NSF).

REFERENCES

1. **Cetinorgu, E., Gumus, C., Esen, R.** Effects of Deposition Time and Temperature on the Optical Properties of Air-annealed Chemical Bath Deposited CdS Films *Thin Solid Films* 515 2006: pp. 1688 – 1693.
2. **Barkat, L., Hamdadou, N., Morsli, M., Khelil, A., Bernede, J. C.** Growth and Characterization of $CuFeS_2$ Thin Films *Journal of Crystal Growth* 297 2006: pp. 426 – 431.
3. **Orts, J. L., Diaz, R., Herrasti, P., Rueda, F., Fatas, E.** $CuInTe_2$ and In-rich Telluride Chalcopyrites Thin Films Obtained by Electrodeposition Techniques *Solar Energy Materials & Solar Cells* 91 2007: pp. 621 – 628.
4. **Gautier, C., Breton, G., Nouaoura, M., Cambon, M., Charar, S., Averous, M.** Sulfide Films on PbSe Thin Layer Grown by MBE *Thin Solid Films* 315 1998: pp. 118 – 122.
5. **Armstrong, S., Datta, P. K., Miles, R. W.** Properties of Zinc Sulfur Selenide Deposited Using a Close-spaced Sublimation Method *Thin Solid Films* 403–404 2002: pp. 126 – 129.
6. **Qasrawi, A. F., Kayed, T. S., Ercan, I.** Fabrication and Some Physical Properties of $AgIn_5S_8$ Thin Films *Materials Science and Engineering* B 113 2004: pp. 73 – 78.
7. **Bedir, M., Oztas, M., Bakkaloglu, O. F., Ormanci, R.** Investigations on Structural, Optical and Electrical Parameters of Spray Deposited ZnSe Thin Films with Different Substrate Temperature *The European Physical Journal* B 45 2005: pp. 465 – 471.
8. **He, Y. B., Polity, A., Alves, H. R., Osterreicher, I., Kriegseis, W., Pfisterer, D., Meyer, B. K., Hardt, M.** Structural and Optical Characterization of RF Reactively Sputtered $CuInS_2$ Thin Films *Thin Solid Films* 403–404 2002: pp. 62 – 65.
9. **Berrigan, R. A., Maung, N., Irvine, S. J. C., Hamilton, D. J. C., Ellis, D.** Thin Films of CdTe/CdS Grown by MOCVD for Photovoltaics *Journal of Crystal Growth* 195 1998: pp. 718 – 724.
10. **Atif, M. A., Takao, I., Seiichi, H.** Structural and Photo-luminescence Properties of Nanocrystalline Silicon Films Deposited at Low Temperature by Plasma-enhanced Chemical Vapor Deposition *Applied Surface Science* 253 2006: pp. 1198 – 1204.
11. **Anuar, K., Zainal, Z., Hussein, M. Z., Saravanan, N., Haslina, I.** Cathodic Electrodeposition of Cu_2S Thin Film for Solar Energy Conversion *Solar Energy Materials & Solar Cells* 73 2002: pp. 351 – 365.
12. **Cheng, S. Y., Chen, G. N., Chen, Y. Q., Huang, C. C.** Effect of Deposition Potential and Bath Temperature on the Electrodeposition of SnS Film *Optical Materials* 29 2006: pp. 439 – 444.
13. **Shen, C. M., Zhang, X. G., Li, H. L.** Effect of pH on the Electrochemical Deposition of Cadmium Selenide Nanocrystal Films *Materials Science and Engineering* B 84 2001: pp. 265 – 270.
14. **Junichi, N., Sunao, C., Yukifumi, U., Yoshio, N.** Electrodeposition Method for Controlled Formation of CdS Films From Aqueous Solutions *Journal of Electroanaytical Chemistry* 473 1999: pp. 217 – 222.
15. **Heini, S., Marianna, K., Mikko, R., Markku, L.** Electrochemical Quartz Crystal Microbalance Study on Cyclic Electrodeposition of PbS Thin Films *Thin Solid Films* 386 2001: pp. 32 – 40.
16. **Li, W. K., Meng, X. T., Liang, X., Wang, H., Yan, H.** Electrodeposition and Characterization of PbSe Films on Indium Tin Oxide Glass Substrates *Journal of Solid State Electrochemistry* 10 2006: pp. 48 – 53.
17. **Zulkarnain, Z., Saravanan, N., Anuar, K., Mohd, Z. H. Wan, M. M. Y.** Effects of Annealing on the Properties of SnSe Films *Solar Energy Materials &Solar Cells* 81 2004: pp. 261 – 268.
18. **Gode, F., Gumus, C., Zor, M.** Investigations on the Physical Properties of the Polycrystalline ZnS Thin Films Deposited by the Chemical Bath Deposition Method *Journal of Crystal Growth* 299 2007: pp. 136 – 141.
19. **Dalchiele, E. A., Cattarin, S., Musiani, M. M.** Preparation of $CdIn_2Se_4$ Thin Films by Electrodeposition *Journal of Applied Electrochemistry* 28 1998: pp. 1005 – 1008.
20. **Pistone, A., Arico, A. S., Antonucci, P. L., Silvestro, D., Antonucci, V.** Preparation and Characterization of Thin Film ZnCuTe Semiconductors *Solar Energy Materials & Solar Cells* 53 1998: pp. 255 – 267.
21. **Subramanian, B., Sanjeeviraja, C., Jayachandran, M.** Materials Properties of Electrodeposited $SnS_{0.5}Se_{0.5}$ Films and Characterization of Photoelectrochemical Solar Cells *Materials Research Bulletin* 38 2003: pp. 899 – 908.
22. **Asenjo, B., Chaparro, A. M., Gutierrez, M. T., Herrero, J.** Electrochemical Growth and Properties of $CuInS_2$ Thin Films for Solar Energy Conversion *Thin Solid Films* 511–512 2006: pp. 117 – 120.
23. **Guillen, C., Martinez, M. A., Herrero, J., Gutierrez, M. T.** Chemical Studies of Solar Cell Structures Based on Electrodeposited $CuInSe_2$ *Solar Energy Materials & Solar Cells* 58 1999: pp. 219 – 224.

DOI: 10.5755/j02.ms.26239